Control Analysis of an Ion Thruster with Programed Thrust

P. A. MUELLER*
Bendix Research Laboratories, Southfield, Mich.

AND

E. V. PAWLIK†
Jet Propulsion Laboratory, Pasadena, Calif.

Results of an analysis and a digital computer simulation of various control loops for ion thruster control are presented. The concept considered for controlling the thrust of an ion thruster over a 2-to-1 range in output power is to vary the propellant flowrate as both the specific impulse and propellant utilization are maintained at constant values. Thrusters employing oxide cathodes and utilizing mercury as propellant are analyzed extensively with a detailed digital computer simulation. It was necessary to use nonoptimum efficiency thruster to obtain a stable system when a propellant flow rate meter is not used. The use of a propellant flow rate meter makes higher thruster efficiencies usable in a stable configuration.

I. Introduction

SEVERAL interplanetary missions using a solar-powered electric propulsion have been studied and, as a result, system requirements have been generated.[1-4] Among some of the system requirements are long life, stable operation, programable power consumption, an accurate definition of propellant utilization, and high efficiency and reliability. The exact numerical values are mission-dependent.

The system aspects of solar-electric missions are being investigated at Jet Propulsion Laboratory (JPL) as part of the Solar-Electric Propulsion System Technology (SEPST) program. The major areas of concern include: 1) thrusters, 2) propellant tankage, 3) power conditioning and controls, 4) load matching and switching, and 5) thrust-vector position control. Progress in some of the areas of the program has been reported elsewhere.[5-7] The specific topic of this paper is the control of the thruster.

The controls are an integral part of the thruster power conditioning. Specific impulse and thrust are directly controlled. The time-variations in thruster components (especially vaporizers and cathodes) make it necessary to use controllers of a closed-loop form.

II. Thruster and Power Conditioning

The control loops investigated are those associated with a 20-cm ion thruster of the type described in Ref. 8. This thruster employs an oxide-coated cathode and operates at a maxium power level of 2.5 kw. This thruster is ideal for analysis and computer simulation. It is quite well understood and documented, and it provides most types of control problems found during thruster operation. Further work in this area might consider the use of a hollow cathode[9] as the electron source since it provides longer thruster lifetime and higher efficiency.

The power conditioning unit for the thruster is comprised of eight power supplies (see Fig. 1). The function of each of the eight power supplies is as follows: V_1—electromagnet (not required if permanent magnets are used) and manifold heater; V_2—vaporizer heater; V_3—thruster cathode heater; V_4—discharge (arc voltage); V_5—screen grid; V_6—accelerator grid; V_7—neutralizer cathode and vaporizer; V_8—neutralizer keeper.

Power matching and other system aspects have been reported.[5,7,10] The data necessary for the present study were obtained through extensive testing of this type of thruster and system.

III. Description of Control Loops

Mission requirements for ion thrusters appear, at this time, to be somewhat restrictive.[2] Thrust accuracies and allowable propellant utilization fluctuations on the order of a few per cent can be expected. These are in addition to the assumed high-efficiency and specific-impulse requirements. The requirements make control of long-life ion thrusters a nontrivial process. The long-life requirement alone imposes the need for closed-loop operation because of time variations in the thruster components. Programable power consumption (over a 2-to-1 range) imposes yet another requirement on the loops. A concept for incorporating programable power consumption into the thruster power conditioning is to operate the thruster at a constant specific impulse, maintain a constant propellant utilization, and program the thrust. Since both power consumption and thrust are approximately proportional to the product of the beam current and the net accelerating voltage, both thrust and power consumption can be controlled (throttled) by varying the beam current while maintaining a constant net acceleration potential.

Mechanization of the aforementioned concept has been studied in detail. In one control scheme the thruster vaporizer is used to control the beam current while in a secondary loop the cathode controls the arc current, thereby compensating for the time-variant properties of the cathode and vaporizer. If these two parameters are uniquely defined, then the propellant utilization is also controlled. Figure 2a indicates the control loop connections for this first case. The screen current is the sum of the beam and accelerator currents.

Presented as Paper 69-239 at the AIAA 7th Electric Propulsion Conference, Williamsburg, Va., March 3-5, 1969; submitted April 4, 1969; revision received February 6, 1970. This paper presents the results of one phase of research carried out at the Jet Propulsion Laboratory, California Institute of Technology, under Contract NAS 7-100, sponsored by NASA.

* Engineer; at the time of the work described in this paper, P. A. Mueller was a NASA Military Detailee assigned to the Jet Propulsion Laboratory.

† Senior Engineer.

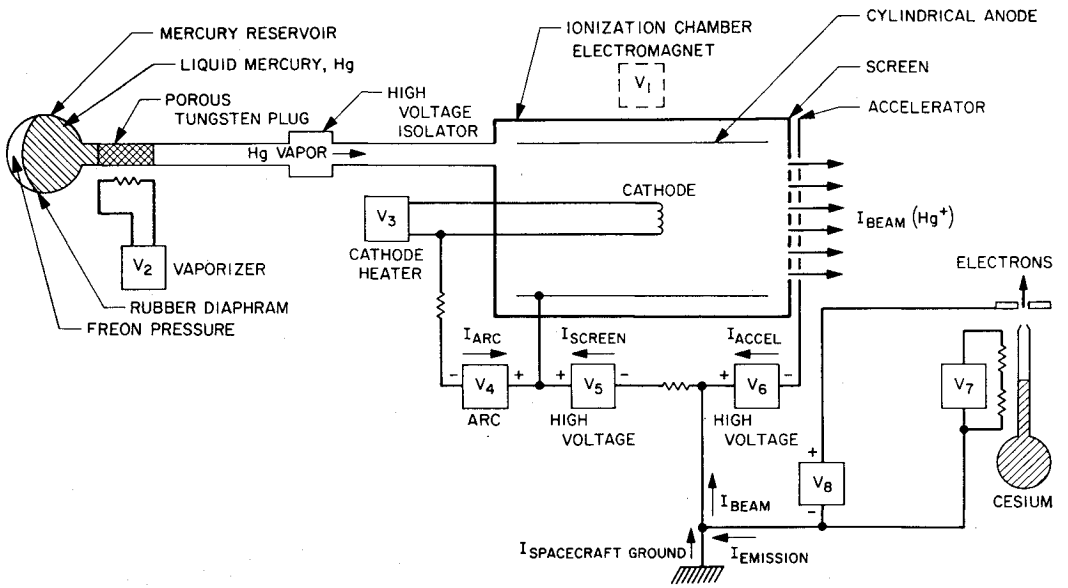

Fig. 1 Ion thruster power conditioning.

Since the accelerator current is on the order of 1% of the screen current, it is often neglected and the times "beam current" and "screen current" can be used synonymously. It should be noted that the beam current reference generates the arc current reference (nonlinear) for the secondary loop. The concept of this scheme may be more readily illustrated by examination of the thrust-chamber characteristics, as shown in Fig. 3.

The combination of a given beam current and a given arc current defines a single point in the characteristic plot. A point on this plot, therefore, specifies a unique propellant utilization, except when the propellant utilization equals unity. The arc current lines do not always have positive slopes, as shown in Fig. 3. The positive slopes for this thruster were obtained by operating at lower magnetic fields than are consistent with minimum arc chamber losses or maximum efficiency.

The control circuitry for the beam current loop is part of the vaporizer supply V_2. The controls for the arc current loop are contained in the cathode heater supply V_3. Supplies V_4, V_5, and V_6 are each maintained at a constant voltage; supply V_1 is held at a constant current. Supplies V_7 and V_8 are used in a third control loop, which operates the cesium neutralizer.

A second means of mechanizing the programable thrust concept is to make use of direct measurement of the propellant mass flowrate. In this manner, both the propellant utilization and the beam current (thrust) can be controlled directly. Figure 2b indicates the control loop connections and the errors that are used to generate corrections in the system outputs. Again, as in the first case, there are both primary and secondary loops. Also, the beam (screen) current reference for the primary loop generates the reference for the secondary loop. In this case, the secondary loop is the mass flowrate loop. The relationship between the beam current and the mass flowrate is an explicit, linear function.

This configuration is more readily controlled because of the irrelevance of the shape of the thruster ion chamber characteristics. A given value of beam current and a given value of mass flowrate always define a unique point on the characteristics.

The loop controls are again located in the power conditioning units. The vaporizer heater supply V_2 controls the propellant mass flowrate. The beam current is controlled by the thruster cathode heater supply V_3. Again, supplies V_4, V_5, and V_6 are held at constant voltage and V_1 is held at a constant current.

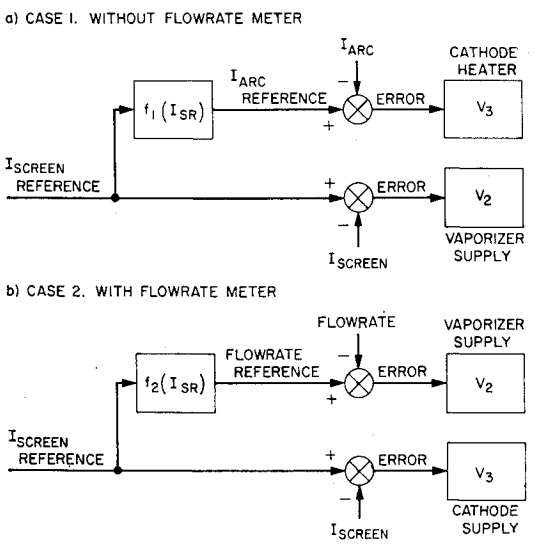

Fig. 2 Ion thruster control loops.

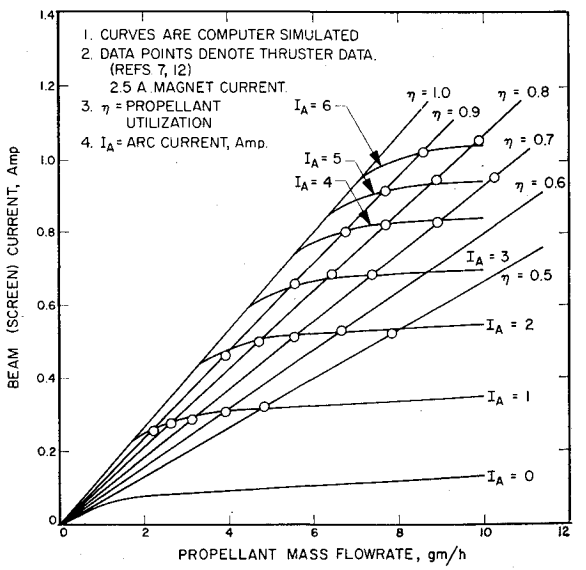

Fig. 3 Thruster ion chamber characteristics.

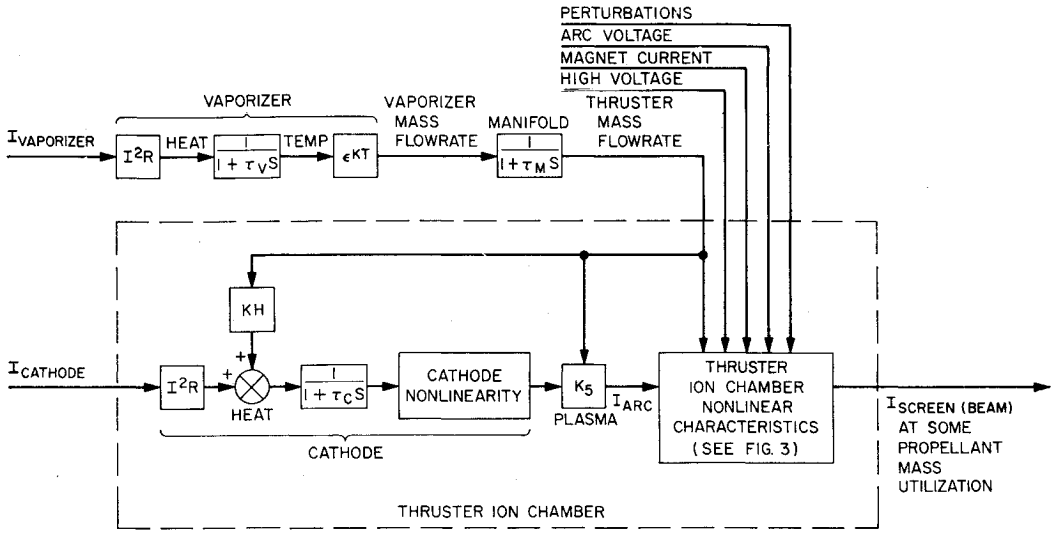

Fig. 4 Ion thruster control block diagram.

IV. Ion Thruster Operation—Analysis and Simulation

Before the inception of this study, some initial work had been performed for control-type analysis of the thruster operation.[11] This work provided a convenient starting point. The primary interrelationships of the thruster components and operational parameters are shown in Fig. 4. An understanding of the control problem requires some familiarity with the control aspects of these interrelationships. Therefore, these control aspects will be treated at this point in the paper.

The propellant feed (vaporizer in Fig. 4) is the only independent function of the thruster system. The current to the vaporizer heater coil heats the porous tungsten plug and vaporizes the mercury propellant. The vaporizer thermal lag is on the order of 100 to 600 sec; it is the primary lag in the system. The temperature-flowrate characteristic is approximated by the exponential function, where K is dependent on the porosity of the plug. The long-term effects on plug porosity are such that the flowrate may decrease by 50% for a given temperature. The volume of the thruster manifold introduces a small (approximately 0.02 sec) lag between the flowrate from the vaporizer surface and that arriving at the thrust chamber. Since the magnitude of this lag is quite small, it can be neglected, and, therefore, no distinction is made when referring to "flow rate."

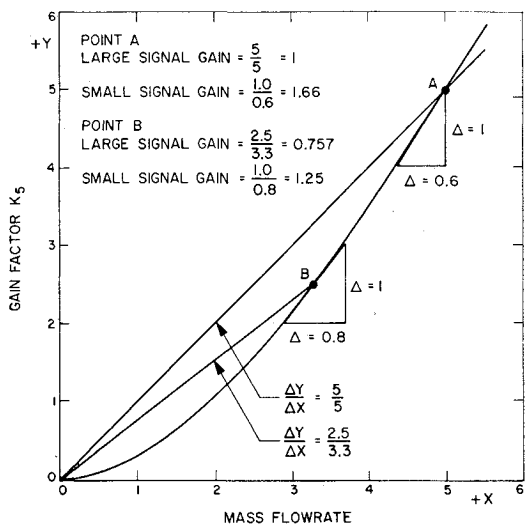

Fig. 5 Illustration of type of nonlinearity in ion thruster control loops.

Inside the ion chamber the functions become more complicated. The cathode has two thermal effects: 1) the effect of the cathode current (predominant effect) and 2) the effect (2 to 4%) of the propellant flowrate (increased ion bombardment at higher plasma densities). The thermal lag is on the order of 120 sec. The plasma is affected by both the cathode temperature and the flowrate, and the arc current is a nonlinear function of those two parameters (as indicated by the block K_5 in Fig. 4). The gain parameter K_5 is a nonlinear function of the mass flowrate and is shaped similar to the curve in Fig. 5.

The combination of the flowrate and the arc current in the thrust chamber can be functionally related to the ion beam current. The thrust-chamber characteristics of Fig. 3 indicate the relationship of the beam current, the arc current, and the propellant mass flowrate. Figure 3 denotes a given (constant) set of values for the supplies V_1, V_4, and V_5 and V_6. Variations in the thruster characteristics will be considered in Sec. VI.

The simulation language used was DSL/90, a language that allows easy digital programing of block diagrams. The language was used on an IBM 7094 computer. The DSL/90 permits use of several integration routines. However, fifth-order Milne Predictor-Corrector routine was selected for these simulations.

The computer simulation includes all effects pertinent to the control of the ion thruster. Several of the blocks in Fig. 4 are written in single statements. This is true of common

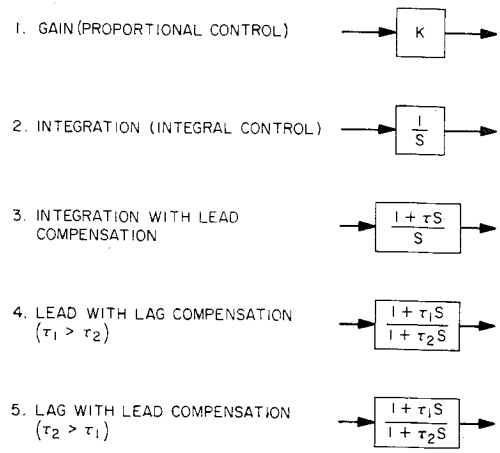

Fig. 6 Controls and transfer functions.

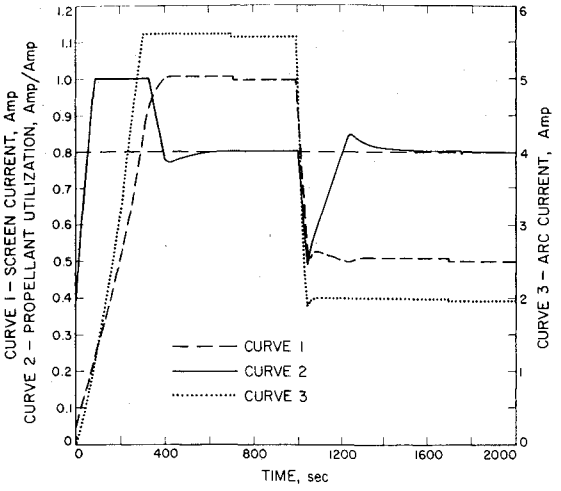

Fig. 7 System responses—without flow rate meter (case 1).

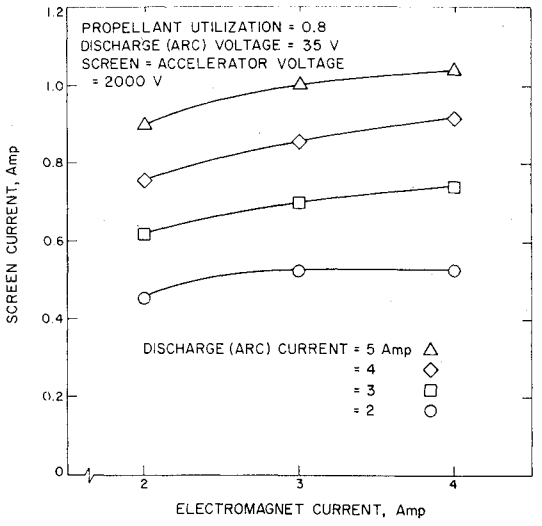

Fig. 9 Perturbation effect of electromagnet current.

functions such as the square, exponential, summation, integration, and limiter functions. Nonlinearities of an empirical-type are programed by inputting the empirical data points and permitting the computer to interpolate linearly between data points. This function generation procedure is used for such functions as the gain factor K_5. The thruster ion chamber nonlinear characteristics are simulated by use of both standard statements and programed function generators. The total system time performance, both closed and open loop, was analyzed.

V. Thruster Control

The goals in the study of the thruster controls were to obtain stable loop and system operation, to determine the necessary controllers for the loops, to determine the errors in controlled parameters, and to simulate the thruster control loops on the digital computer. Also under consideration were perturbations of the system by degradation of components and variations in fixed-value power supplies.

Several controllers of a classical form were investigated and simulated with the ion thruster control loops. These controllers, and their transfer functions, are presented in Fig. 6.

Two control problems were considered: 1) thruster control without use of a propellant mass flowrate meter and 2) control utilizing the flowrate meter (see Fig. 2). Selection of loop control for case 1 started with a preliminary analysis which utilized linear approximations of the control loops and ignored

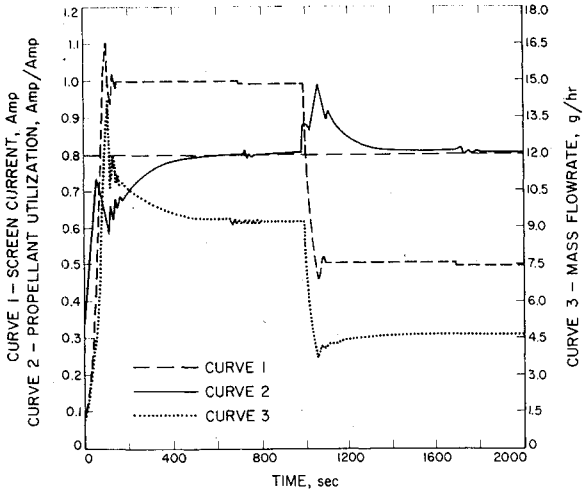

Fig. 8 System responses—with flow rate meter (case 2).

the loop interactions. Straight-line approximations were made for the thruster ion chamber characteristics. The slopes of the characteristics were taken at a propellant utilization of 0.8. This value was chosen because it appeared to be the over-all optimum point for thruster operation in view of thruster efficiency and control and cathode lifetime. The linearization made possible the use of Bode plots for preliminary investigation. A vaporizer time constant of 600 sec and a cathode time constant of 120 sec were assumed. These assumptions neglected both the manifold lag of 0.02 sec and the lags of the power conditioning, which were estimated to be from 1 to 20 msec.

Linearization made it appear that beam current errors could be reduced by use of sufficiently high loop gain. However, results of more detailed analysis proved this assumption to be incorrect. The reasons for this fallacy are the two considerations ignored in the linearization, i.e., the nonlinearity of the system and the interaction of the two loops.

Figure 5 demonstrates the effect of a typical nonlinearity. The difference between the large signal and the small signal gains at point A should be noted. This effect in the thruster loops causes the two gains to differ by as much as an order of magnitude. Also, the difference between the large signal gains at points A and B should be noted. This effect appears in the thruster loops as the result of throttling and the changing of thruster set points by a 2-to-1 ratio. The throttling effect is also the predominant interloop effect.

The large signal gain of the system is the simple ratio of output to input. Since the system output cannot exceed the capabilities of the power supplies, the large signal gain is bounded by the power supply limitations. The small signal gain is the ratio of a small change in output to a small change in input at some particular operating point. If the small signal gain is higher than the large signal gain, instability can occur, causing an oscillation whose amplitude is limited only by the lower value of the large signal gain. The result is a local oscillation at the operating point. If the small signal gain is not high enough to cause an oscillation, it may still cause dynamic effects, such as overshoot which dampens out only after several cycles.

The gain consideration led to conflicts between error criteria and stability criteria. Integral control was considered as a means of reducing the gain requirements and obtaining the zero output error associated with integral control. Use of integral control to meet both criteria resulted in the need for low loop gain for stability and subsequent excessively long time response. The response of the system became bounded by the integrator control instead of by the existing power supply limitation bound.

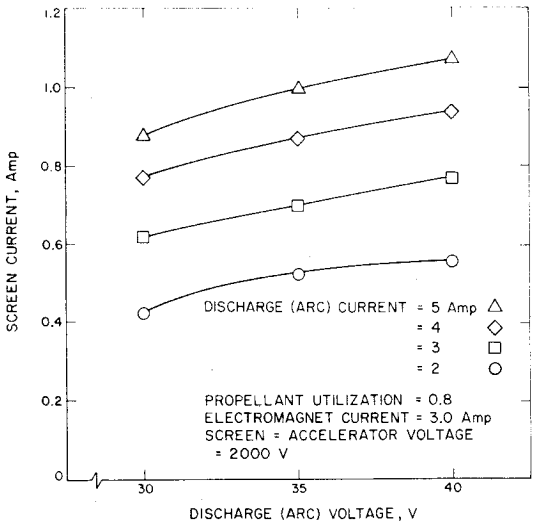

Fig. 10 Perturbation effect of discharge (arc) voltage.

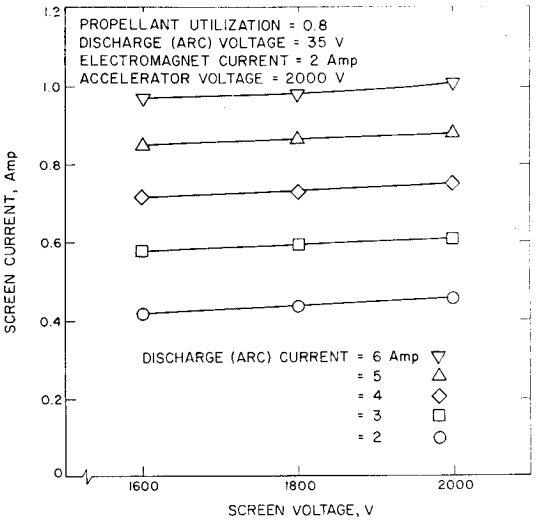

Fig. 11 Perturbation effect of screen voltage.

A controller that accomplished both good dynamic response and small output error is the integral with lead compensation controller. This device can be mechanized in circuitry by paralleling an amplifier with an integrator and summing their outputs. The amplifier thus gives the gain for the dynamic response while the integrator gives potential for zero output error in the system. Figure 7 shows the time response of the system with all nonlinearities included. The screen current reference is varied in several steps. The initial value is 1.000 amp. It decreases to 0.995 at 700 sec, 0.500 at 900 sec, and 0.495 at 1700 sec. The propellant utilization set point is 0.80. After the transients die out the screen current and the propellant utilization are at the desired values. These results are for the case of a new cathode and a new vaporizer. Results for degraded components differ only slightly.

Other controllers were also considered; however, it was felt that integral control of some sort was needed because of tight requirements on the beam current and utilization. It should be noted that the ion chamber characteristics have constant arc current curves of very slight slope. Small errors in either arc or beam current cause the operating point to shift from the desired propellant utilization point. Perturbations of the system power conditioning units cause a similar type of effect on the utilization and will be considered in Sec. VI.

Investigation of thruster control using a propellant mass flowrate meter (case 2) began with the experience gained in case 1. New constraints were imposed, the first being that of the expected form of the flowrate meter. The assumed specification was 1% accuracy with a time lag of 10 sec. A reduction of the vaporizer time constant from 600 to 120 sec was assumed. Beam current accuracy was selected as 1%. An attempt was made to minimize the complexity of the controls in this case. It was soon found that simple gain in the screen loop and lag with lead compensation in the flowrate loop would be sufficient. Figure 8 shows the time response of the system with all nonlinearities included. Again, the screen reference was stepped to show response to large and small signals.

VI. Perturbation Effects

In addition to the investigation of the degradation effects of the cathode and vaporizer, perturbations of power con-

Table 1 Effects of perturbations up to 2% on propellant utilization

Case	Screen current, Amp	Parameter	Propellant utilization at perturbation levels														
			+2%	+0.5%	0	-0.5%	-2%	+2%	+0.5%	0	-0.5%	-2%	+2%	+0.5%	0	-0.5%	-2%
1	1.0	Electromagnet current	0.841	0.812	0.800	0.789	0.756	0.886	0.860	0.850	0.840	0.811	0.909	0.902	0.900	0.898	0.891
		Discharge (arc) voltage	0.891	0.830		0.769	0.675	0.902	0.878		0.824	0.728	0.926	0.906		0.893	0.842
		Screen voltage	0.836	0.810		0.790	0.762	0.884	0.858		0.842	0.818	0.908	0.902		0.898	0.893
		Arc current reference	0.889	0.828		0.772	0.685	0.900	0.875		0.826	0.739	0.924	0.906		0.894	0.850
	0.5	Electromagnet current	0.806	0.802	0.800	0.798	0.793	0.858	0.852	0.850	0.848	0.842	0.907	0.902	0.901	0.900	0.895
		Discharge (arc) voltage	0.818	0.804		0.795	0.741	0.872	0.855		0.845	0.829	0.917	0.905		0.897	0.881
		Screen voltage	0.812	0.803		0.797	0.767	0.864	0.853		0.847	0.837	0.911	0.903		0.898	0.890
		Arc current reference	0.825	0.806		0.794	0.714	0.873	0.856		0.844	0.828	0.918	0.905		0.897	0.880
2	1.0	Propellant mass	0.786	0.798	0.802	0.806	0.818	0.835	0.848	0.852	0.857	0.870	0.885	0.898	0.903	0.907	0.921
	0.5	Flowrate reference	0.787	0.799	0.803	0.807	0.820	0.837	0.849	0.854	0.858	0.871	0.886	0.899	0.904	0.908	0.922

ditioning were studied. The perturbations affect the thruster ion chamber nonlinear characteristics (Fig. 3) and the references for the secondary loops in cases 1 and 2.

The perturbation of the secondary reference loop is an important consideration in case 1 where the reference has a nonlinear characteristic and is more susceptible to drift, etc., than the single-valued reference in case 2. Similarly, perturbation of the regulated supplies of the power conditioning has quite an effect in case 1, but one of little control significance in case 2. The regulated supplies are V_1, V_4, V_5, and V_6. Perturbations of the supplies cause a change in the spacing of the constant arc curves in the ion chamber characteristics. Figures 9, 10, and 11 were generated from engine performance data[7,12] and illustrate the perturbation effects. A quantitative evaluation of these curves leads to the formulation of a perturbation factor for each of the three effects.

These perturbations were applied to the simulation to determine the effects in the system performance. Only the reference perturbation was considered for the case 2 since the supply variations do not affect the operation when a flowrate meter is used. Table 1 lists the results for 0.5 and 2% perturbations of the references and supplies.

The table's columns for zero perturbation exemplify the accuracy with which utilization can be controlled with the complex controllers of case 1. Likewise, the same data show the effects of relaxed specifications in case 2. Errors caused by $\pm 0.5\%$ perturbations decrease with increasing propellant utilization set points. This can be attributed to higher slope of the constant arc current curves at the higher utilizations. Discharge (arc) voltage perturbations caused the greatest utilization errors. The one point of comparison between cases 1 and 2 is the error due to perturbations of the reference. Case 2 proves to be affected less than case 1. As previously noted, the reference of case 2 is also less subject to drift, offset, etc., since it is a single-valued function.

VII. Conclusions and Comments

From this study of ion thruster controls, it can be concluded that stable operation is feasible with realistic controllers. However, the control mode which does not make use of a propellant mass flowrate meter is restricted in several ways. In particular, thrusters need to be operated at nonoptimum efficiency to obtain positive sloping thruster ion chamber characteristics. Also, this control mode is susceptible to errors in regulated power supplies and in arc reference function generators. The problem can be partly alleviated by operating at higher utilization, but this could possibly be in conflict with requirements for long-life cathodes. Power conditioning specifications can also be made more stringent, but certainly only with a penalty in complexity and weight. As a result of investigation of controls that utilize a propellant flowrate meter, it can be concluded that this control mode is more desirable than the previous mode. Incorporation of such a flowrate device within a system is a possible improvement. Such a device, however, is not a panacea. If the beam current and the propellant utilization are closely regulated, the thrust and power consumption can still vary by an amount proportionate to errors in the screen high voltage. These points deserve renewed investigation from both the power conditioning and the mission aspects.

References

[1] Stearns, J. W. and Kerrisk, D. J., "Solar-Powered Electric Propulsion Engineering and Applications," AIAA Paper 66-576, Colorado Springs, Colo., 1966.

[2] "1975 Jupiter Flyby Mission Using a Solar Electric Propulsion Spacecraft," Internal Report, March 1968, Jet Propulsion Lab., Pasadena, Calif.

[3] Kerrisk, D. J. and Kaufman, H. R., "Electric Propulsion for Primary Spacecraft Propulsion," AIAA Paper 67-424, Washington, D. C., 1967.

[4] Kerrisk, D. J. and Bartz, D. R., "Primary Electric Propulsion Systems Technology and Applications," *Astronautics and Aeronautics*, Vol. 6, No. 6, June 1968, pp. 48–53.

[5] Pawlik, E. V., Macie, T. W., and Ferrera, J. D., "Electric Propulsion System Performance Evaluation," AIAA Paper 69-236, Williamsburg, Va., March 1969.

[6] Masek, T. D., "Experimental Studies with a Mercury Bombardment Thruster System," TR 32-1280, July 15, 1968, Jet Propulsion Lab., Pasadena, Calif.

[7] Masek, T. D. and Pawlik, E. V., "Thrust System Technology for Solar Electric Propulsion," AIAA Paper 68-541, Cleveland, Ohio, 1968.

[8] Masek, T. D., "Evaluation of the SE-20C Thruster Design," *Space Programs Summary 37-51*, Vol. III, June 30, 1968, Jet Propulsion Lab., Pasadena, Calif.

[9] Byers, D. C. and Staggs, J. F., "SERT II Flight-Type Thruster System Performance," AIAA Paper 69-235, Williamsburg, Va., 1969.

[10] Pawlik, E. V., "Power Matching of an Ion Thruster to Solar Cell Power Output," TM 33-392, June 1968, Jet Propulsion Lab., Pasadena, Calif.

[11] Pawlik, E. V., Nakanishi, S., and Alegri, H. R., "Some Dynamic Characteristics of an Electron-Bombardment Ion Thruster," TN D-4204, Oct. 1967, NASA.

[12] Masek, T. D., unpublished data, 1968, Jet Propulsion Lab., Pasadena, Calif.